Title

Genomic Architecture of Hybrid Male Sterility in a Species Without Sex Chromosomes (Tigriopus californicus, Copepoda: Harpacticoida)

Journal

Genome Biology and Evolution, 15(6)

ISSN

1759-6653

Authors

Olsen, Kevin C
Lima, Thiago G
Barreto, Felipe S
et al.

Publication Date

2023-06-01

DOI

10.1093/gbe/evad091

Title: Genomic architecture of hybrid male sterility in a species without sex chromosomes (*Tigriopus californicus*, Copepoda: Harpacticoida)

Authors: Kevin C. Olsen[1*], Thiago G. Lima[1], Felipe S. Barreto[2], and Ronald S. Burton[1]

Affiliations:

[1]University of California San Diego, Scripps Institution of Oceanography Marine Biology Research Division, CA, USA

[2]Oregon State University, Department of Integrative Biology, OR, USA

Corresponding Author Email: * k.olsen.ecoevo@gmail.com

Author Contributions:

TGL and RSB conceived the study. TGL performed laboratory and bioinformatic processing. KCO and FSB conducted statistical analyses. KCO wrote the manuscript. All authors contributed to interpreting results and editing the manuscript.

Conflict of Interest Statement:

The authors declare there is no conflict of interest.

Acknowledgements:

This work was supported by the NSF Postdoctoral Research Fellowships in Biology Program with awards to KCO (2109676), TGL (1523543) and NSF grants DEB-1556466 and IOS-1754347 to RSB.

Abstract

Sterility among hybrids is one of the most prevalent forms of reproductive isolation delineating species boundaries and is expressed disproportionately in heterogametic XY males. While hybrid male sterility (HMS) due to the 'large X effect' is a well-recognized mechanism of reproductive isolation, it is less clear how HMS manifests in species that lack heteromorphic sex chromosomes. We evaluated differences in allele frequencies at approximately 460,000 SNPs between fertile and sterile F_2 interpopulation male hybrids to characterize the genomic architecture of HMS in a species without sex chromosomes (*Tigriopus californicus*). We tested associations between HMS and mitochondrial-nuclear and/or nuclear-nuclear signatures of incompatibility. Genomic regions associated with HMS were concentrated on a single chromosome with the same primary 2 Mbp region identified in one pair of reciprocal crosses. Gene Ontology analysis revealed that annotations associated with spermatogenesis were the most overrepresented within the implicated region, with 9 protein-coding genes connected with this process found in the QTL of chromosome 2. Our results indicate that a narrow genomic region was associated with the sterility of male hybrids in *T. californicus* and suggest that incompatibilities among select nuclear loci may replace the large X effect when sex chromosomes are absent.

Keywords: Hybrid male sterility, reproductive isolation, Pool-seq, *Tigriopus californicus*

Significance Statement

Reproductive incompatibility between divergent taxa can often be traced to hybrid male sterility. For many animals, hybrid male sterility is due to genetic incompatibilities associated with sex chromosomes. Yet not all species have sex chromosomes. In these species, sterility might be due

to incompatibilities between mitochondrial and nuclear genes or strictly among nuclear genes themselves. We evaluated the causes of hybrid sterility in a copepod species without sex chromosomes and found that incompatibilities underlying sterility map to a single autosome where genes involved with spermatogenesis are enriched and are likely involved in male reproductive failure. Our results highlight how hybrid male sterility and the boundaries between species may be maintained through population-specific nuclear incompatibilities in taxa without sex chromosomes.

Introduction

Inviability and reproductive failure in interspecific hybrids can often be attributed to mismatching genetic elements with differing evolutionary histories (Dobzhansky 1936; Muller 1942; Orr 1995). Incompatibilities among sex and autosomal chromosomes make an especially strong contribution to hybrid reproductive failure and the formation of allopatric species (*i.e.*, the 'Large X Effect; Presgraves 2008; Phillips and Edmands 2012; Lima 2014). In many interspecific crosses, hybrid offspring that are members of the heterogametic sex are more susceptible to reproductive failure than their homogametic counterparts (Haldane 1922). 'Haldane's Rule' can often be attributed to recessive sex-linked factors that are hidden in homogametic individuals but exposed in heterogametic form (Turelli and Orr 1995; Presgraves and Orr 1998). Sterility is one such hybrid incompatibility that is disproportionately prevalent in males (or females in ZW systems), typically because of genetic elements that accumulate on sex chromosomes (Price and Bouvier 2002; Masly and Presgraves 2007; Presgraves and Meiklejohn 2021). In fruit flies, nematodes, mosquitos, and mice, hybrid male sterility (HMS) can be traced to incompatibilities between X-linked and autosomal loci (Tao et al. 2003; Slotman et al. 2004;

Schwann et al. 2018; Bi et al. 2019). While the concept of the large X effect has a broad influence, it is not well understood how HMS manifests across animal species that lack sex-determining chromosomes or have a strong environmental contribution to sex determination (Moyle and Graham 2005; Moyle and Nakazato 2008; Willett 2008).

Aside from sex chromosomes, incompatibilities between nuclear and mitochondrial genomes are at times linked to male sterility in plants and hybrid inviability across taxa (Chase 2007; Burton et al. 2013). In many angiosperms, sterility-causing mutations involve new open reading frames (ORFs) formed from recombining mitochondrial genomes, but these mutations are often counteracted by nuclear 'restorer-of-fertility' genes (Chase 2007; Case and Willis 2008). Moreover, mito-nuclear interactions play an important role in the fitness breakdown of interpopulation or interspecific F_2 hybrids in some animal and fungal taxa (Bolnick et al. 2008; Chou et al. 2010; Meiklejohn et al. 2013; Lima et al. 2019; Healy and Burton 2020). Hybrid breakdown due to mito-nuclear interactions in these systems is most often manifested via inviability, slow development, metabolic dysfunction, and smaller clutch sizes. Alternatively, incompatibilities strictly among nuclear autosomal loci contribute to hybrid pollen sterility in some hermaphroditic plants (Sweigart et al. 2006; Long et al. 2008; Feng et al. 2020), but the pervasiveness of this pattern in species with separate male and female sexes is uncertain. Assessing the genomic architecture of HMS in species with separate sexes but without sex chromosomes could provide valuable insight to the relative importance of nuclear and mito-nuclear interactions in the formation of reproductive isolation generally and HMS in particular.

We evaluated the genomic architecture of male sterility resulting from interpopulation hybridization in the tidepool copepod *Tigriopus californicus*. *T. californicus* has a polygenic sex-determining system and lacks heteromorphic sex chromosomes (Alexander et al. 2014; 2015). In

some interpopulation crosses, male sterility in F_2 hybrids is increased relative to its baseline frequency within populations (Willett 2008). In the absence of sex chromosomes, asymmetries in the manifestation of HMS between reciprocal crosses might implicate mito-nuclear incompatibilities as an important source of sterility. Alternatively, HMS in *T. californicus* could be the result of mismatches among nuclear elements and these effects may be localized or dispersed throughout the genome.

Results

In reciprocal crosses between copepods from Abalone Cove (AB) and San Diego (SD) CA, USA, we scored fertility and sterility across a total of ~2000 F_2 interpopulation male hybrids, and then performed whole-genome sequencing of four pools (*i.e.,* a pool of fertile males and a pool of sterile males for each cross direction). Allele frequencies in AB♀ x SD♂ and SD♀ x AB♂ crosses were evaluated at 462,330 and 458,526 population-diagnostic SNPs, respectively (Table S1). The average depth of coverage per locus ranged from 68.824 ± 0.100 (mean ± 95% C.I.) to 85.975 ± 0.159 across the four hybrid pools. The allele frequencies of each pool are plotted in Fig.1.

Regions of the genome associated with HMS were identified by quantifying differences in allele frequencies among fertile and sterile males within each of the reciprocal crosses using a bulk segregant / quantitative trait locus (QTL) approach. G' analyses detected a single 15 Mbp segment on chromosome 2 that was associated significantly with HMS (Fig. 2). Within the region detected in G' analyses, we identified three 2 Mbp QTL peaks where differences in allele frequencies were greatest: *QTL-1* (0.8 – 2.4 Mbp), *QTL-2* (3.4 – 5.7 Mbp), and *QTL-3* (6.2 – 7.6

Mbp) (Fig. 2, Fig. S1). The segment corresponding to *QTL-2* expressed the largest difference in allele frequencies between fertile and sterile male hybrids relative to the rest of the genome, and it overlapped fully between the reciprocal crosses.

A primary goal of this experiment was to assess the potential role of mito-nuclear incompatibilities as a source of HMS. Such incompatibilities would be inferred if sterile males showed patterns of mismatched nuclear allele frequency relative to their respective mitochondrial backgrounds. In other words, sterile males from the AB♀ x SD♂ cross would have elevated SD nuclear allele frequencies, while sterile males from the SD♀ x AB♂ cross would show elevated AB nuclear allele frequencies. Within the detected QTLs, however, sterile males from both cross directions showed elevated frequencies of SD alleles, clearly rejecting the mito-nuclear incompatibility hypothesis for HMS in hybrids between these populations of *T. californicus* (Fig. 1).

We identified 121, 279, and 173 protein-coding genes within *QTL-1*, *QTL-2*, and *QTL-3*, respectively (Table S2). Across the protein-coding genes within the three QTL regions, a total of 55 Gene Ontology terms were overrepresented relative to their frequencies in the whole genome (Table 1; Table S3). Interestingly, the most overrepresented term was 'spermatogenesis', with 9 genes in *QTL-2*, which is ~4.1x more common than expected by chance when considering that 107 total genes are annotated with this GO term.

Discussion

We found a 2 Mbp genomic region closely associated with the sterility of *T. californicus* F_2 interpopulation male hybrids. The boundaries of the region were remarkably consistent in

reciprocal crosses and, unlike other forms of hybrid breakdown in *T. californicus*, displayed patterns indicative of nuclear rather than mito-nuclear incompatibility. Our results suggest mismatches among select nuclear loci were responsible for the sterility of male hybrids and point to the role of autosomal incompatibilities in forming HMS when sex chromosomes are not an available target of intrinsic reproductive isolation.

Within the identified QTL, sterile F_2 male hybrids showed elevated frequencies of SD alleles in both cross directions (Fig. 1), indicating some incompatibility between these SD alleles and nuclear components of the AB genome. In characterizing the frequency of HMS in *T. californicus*, Willett (2008) found that crosses between AB females and SD males had higher occurrence of F_2 male sterility by 11-21% compared with parental populations. Furthermore, sterility was infrequent in F_1 hybrids and crosses between either AB or SD and other populations did not lead to F_2 HMS (Willett 2008). These phenotypic patterns suggest AB and SD genetic elements are particularly prone to forming male sterility when recombined in F_2 hybrids. Given that within the QTL the frequency of AB alleles in sterile males averaged < 0.3 (as opposed to the 0.5 expectation for all alleles in the F_2 generation), we can infer a very strong effect at one or more genes in this region; indeed, if all SD homozygotes are sterile and heterozygotes are unaffected, we would expect an AB frequency of 0.33. Taken together with the Gene Ontology enrichment analysis (Table 1), our results suggest that deleterious interactions among SD and AB nuclear elements on chromosome 2 disrupt spermatogenesis and culminate in hybrid male sterility.

The genetic basis of HMS differs from other forms of F_2 hybrid breakdown and inviability in *T. californicus* (Burton and Barreto 2012; Lima et al. 2019; Healy and Burton 2020; Han and Barreto 2021). While mito-nuclear incompatibilities are disproportionately

responsible for reductions in developmental rate, survivorship, and salinity tolerance in *T. californicus* F_2 hybrids (Burton 1987; Burton 1990a; Burton 1990b; Edmands 1999), no mito-nuclear signature was associated with HMS. A similar pattern has been described in *Caenorhabditis* nematodes, where incompatibilities between mtDNA and nuclear genes contribute to hybrid inviability, but male sterility is the result of a single X-autosome incompatibility (Bundus et al. 2018). Because the AB and SD populations do not show evidence of HMS when crossed to other populations (Willett 2008), the genomic architecture of HMS appears to be more complex in *T. californicus* and involves population-specific interacting elements. This pattern is more akin to polygenic X-autosome interactions described in *Drosophila* clades (Presgraves and Meiklejohn 2021), and epistatic incompatibilities among autosomal loci in some plant taxa that culminate in HMS (Sweigart et al. 2006; Long et al. 2008; Feng et al. 2020). Overall, our results suggest that in some instances without sex chromosomes, nuclear incompatibilities on a single chromosome may make a disproportionate contribution to forming hybrid male sterility and in delineating species boundaries.

Methods

Interpopulation crosses and identification of fertile and sterile male hybrids

Tigriopus californicus were collected from intertidal rocky pools in Abalone Cove (AB; 33°44’ N, 118°22’ W) and San Diego (SD; 32°44’ N, 117°15’ W), CA. Copepods were maintained in mass cultures in 400 mL of 35 ppt seawater and fed ground commercial fish food and natural algal growth. Cultures were kept in incubators at 20°C with a 12-h light/dark cycle. Males and females used in interpopulation crosses were sampled from different mass cultures so

that replicate crosses reflected as much of the genetic variation present in parent populations as possible. Forty-eight reciprocal crosses between AB and SD were established in 24-well culture plates, with a single male-female pair in each well. The resulting F_1 interpopulation hybrids were separated as juveniles and raised to maturity in isolation. F_1 x F_1 crosses were conducted with a single pair per well, with an effort to maximize mixing of offspring from different parental population crosses (*i.e.*, no sibling crosses were performed).

The fertility of F_2 interpopulation male hybrids was assessed by pairing them with a single female in two sequential trials. Females used to assess male fertility were from the population that matched the hybrid male's mitochondrial background. Approximately 1000 F_2 male hybrids were evaluated for both cross directions. We incorporated two classes of F_2 male hybrids: a) Fertile males, which successfully produced offspring in both sequential trials, and b) Sterile males, which failed to produce offspring in both trials. Males that produced offspring with only one of the two females were excluded from the study.

DNA isolation and sequencing

We collected fertile and sterile F_2 hybrid males from both of the reciprocal crosses resulting in four pools: Fertile F_2 males from AB♀ x SD♂ crosses (n = 100), Sterile F_2 males from AB♀ x SD♂ crosses (n = 88), Fertile F_2 males from SD♀ x AB♂ crosses (n = 100), and Sterile F_2 males from SD♀ x AB♂ crosses (n = 76). DNA was isolated using a phenol:chloroform protocol (Sambrook and Russell 2006). Each pool was sequenced as 100-bp paired end (PE) libraries on the Illumina HiSeq 2000. Adapters were trimmed with Trimmomatic (Bolger et al. 2014) and only reads of at least 50-bp were kept after trimming.

SNP database between parental populations

Tigriopus californicus has a reference genome that was developed *de novo* for the SD population where greater than 90% of the genome is anchored to 12 chromosomes (Barreto et al. 2018). Lima et al. (2019) generated an AB consensus genome by mapping AB reads from Lima and Willett (2018) to the most recent SD reference (GenBank accession: GCA_007210735.1). Furthermore, Lima and Willett (2018) and Lima et al. (2019) identified population-diagnostic SNPs for SD and AB. These original analyses were conducted with depth of coverage of ~40X and with reads sequenced from large pools of individuals from SD and AB (~3000 and ~300, respectively) (GenBank accessions SD: SRX469409; AB: SRX2746703). Briefly, the SNP list was developed by (a) performing reciprocal mapping of reads of a population to the reference sequence of the other, (b) considering only those positions where all mapped reads showed an alternative nucleotide to the reference (*i.e.*, fixed differences), and (c) comparing the reciprocal mappings and keeping only SNPs that were fixed differences in both mappings (Lima and Willett 2018). Here we used the SD and AB assemblies and the population-diagnostic SNPs developed by the previous authors.

In the current study, reads from the four hybrid pools were mapped reciprocally to both the SD and AB reference using BWA with default parameters (Li and Durbin 2009), and only reads that mapped with a MAPQ score >20 were kept. PoPoolation2 (Kofler et al. 2011) was used to find positions across the genome where all reads had an alternative nucleotide to that of the reference, considering only biallelic positions with total coverage ≥80 and ≤ 400. Read counts for every variable position were determined using PoPoolation2 (Kofler et al. 2011). Allele frequencies were calculated as the AB allele frequency in reciprocal crosses.

Identification of regions associated with hybrid male sterility

To assess the genomic architecture underlying HMS in *T. californicus*, we evaluated the allele frequency distributions of fertile and sterile F_2 hybrid males with a twostep approach. First, we identified regions of the genome associated with HMS by quantifying differences in allele frequencies among fertile and sterile males within each of the reciprocal crosses (fertile vs. sterile AB♀ x SD♂; fertile vs. sterile SD♀ x AB♂) using a quantitative trait locus (QTL) approach in R 4.1.2 with the package 'QTLseqr' (Mansfeld and Grumet 2018). We estimated the G' statistic described by Magwene et al. (2011) for analyzing bulk segregant data from next generation sequencing under the default settings of the package and 1 Mbp nonoverlapping sliding windows. Varying window size (250 kb - 1Mbp) did not qualitatively change our results. Second, we distinguished the effects of nuclear and mito-nuclear incompatibilities on HMS within these regions by evaluating allele frequency patterns among reciprocal crosses. We expected that if HMS was caused by incompatibilities between nuclear factors, that allele frequencies in sterile males would be shifted in the same direction in both crosses. On the other hand, incompatibilities between the nuclear and mitochondrial genomes would be expected to skew allele frequencies toward the population that matched the mitochondria (see Lima et al. 2019; Pereira et al. 2021).

Enrichment analysis

We used Gene Ontology annotations (GO terms) to search for functional categories that were overrepresented in genomic regions associated with HMS. We focused on three 2Mbp QTLs where differences in allele frequencies between fertile and sterile hybrid males were greatest and compiled gene identifications within these regions with Integrative Genomics Viewer (IGV) (Thorvaldsdottir et al. 2013). We used a Fisher's exact test in the R package 'topGO' (Alexa and

Rahnenfuhrer 2021) to identify GO terms that were overrepresented compared with the rest of the genome and report only those with $p \leq 0.01$ and at least 10 genomic annotations.

Data accessibility statement:

The data supporting this article are available in NCBI's Sequence Read Archive (SRA) under accession numbers SRR24623753-SRR24623756.

References:

Alexa, A., and J. Rahnenfuhrer. 2021. topGO: Enrichment analysis for gene ontology. R package version 2.46.0.

Alexander, H.J., J.M.L. Richardson, and B.R. Anholt. 2014. Multigenerational response to artificial selection for biased clutch sex ratios in *Tigriopus californicus*. J. Evol. Biol. 27: 1921-1929.

Alexander, H.J., J.M.L. Richardson, S. Edmands, and B.R. Anholt. 2015. Sex without sex chromosomes: genetic architecture of multiple loci independently segregating to determine sex ratios in the copepod *Tigriopus californicus*. J. Evol. Biol. 28: 2196-2207.

Barreto, F.S., E.T. Watson, T.G. Lima, C.S. Willett, S. Edmands, W. Li, and R.S. Burton. 2018. Genomic signatures of mitonuclear coevolution across populations of *Tigriopus californicus*. Nat. Ecol. Evol. 2: 1250-1257.

Bi, Y., X. Ren, R. Li, Q. Ding, D. Xie, and Z. Zhao. 2019. Specific interactions between autosome and X chromosomes cause hybrid male sterility in *Caenorhabditis* species. Genetics 212: 801-813.

Bolger, A.M., M. Lohse, and B. Usadel. 2014. Trimmomatic: a flexible trimmer for Illumina sequence data. Bioinformatics 30: 2114-2120.

Bolnick, D.I., M. Turelli, H. Lopez-Fernandez, P.C. Wainwright, and T.J. Near. 2008. Accelerated mitochondrial evolution and 'Darwin's corollary': asymmetric viability of reciprocal F1 hybrids in centrarchid fishes. Genetics 178: 1037-1048.

Burton, R.S. 1987. Differentiation and integration of the genome in populations of the marine copepod *Tigriopus californicus*. Evolution 41: 504-513.

Burton, R.S. 1990a. Hybrid breakdown in developmental time in the copepod *Tigriopus californicus*. Evolution 44: 1814-1822.

Burton, R.S. 1990b. Hybrid breakdown in physiological response: a mechanistic approach. Evolution 44: 1806-1813.

Burton, R.S., and F.S. Barreto. 2012. A disproportionate role for mtDNA in Dobzhansky-Muller incompatibilities? Mol. Ecol. 21:4942-4957.

Burton, R.S., R.J. Perieira, and F.S. Barreto. 2013. Cytonuclear genomic interactions and hybrid breakdown. Annu. Rev. Ecol. Evol. Syst. 44: 281-302.

Bundus, J.D., D. Wang, and A.D. Cutter. 2018. Genetic basis to hybrid inviability is more complex than hybrid male sterility in *Caenorhabditis* nematodes. Heredity 121: 169-182.

Case, A.L., and J.H. Willis. 2008. Hybrid male sterility in *Mimulus* (Phrymaceae) is associated with a geographically restricted mitochondrial rearrangement. Evolution 62: 1026-1039.
Chase, C.D. 2007. Cytoplasmic male sterility: a window to the world of plant-mitochondrial interactions. Trends Genet. 23: 81-90.
Chou, J., Y. Hung, K. Lin, H. Lee, and J. Leu. 2010. Multiple molecular mechanisms cause reproductive isolation between three yeast species. PLoS Biol. 8: e1000432–125.
Dobzhansky, T. 1936. Studies on hybrid sterility. II. Localization of sterility factors in *Drosophila pseudoobscura* hybrids. Genetics 21: 113-135.
Edmands, S. 1999. Heterosis and outbreeding depression in interpopulation crosses spanning a wide range of divergence. Evolution 53: 1757-1768.
Feng, C., H. Yi, L. Yang, and M. Kang. 2020. The genetic basis of hybrid male sterility in sympatric *Primulina* species. BMC Evol. Biol. 20: 49.
Haldane, J.B.S. 1922. Sex ratio and unisexual sterility in animal hybrids. J. Genet. 12: 101-109.
Han, K-L., and F.S. Barreto 2021. Pervasive mitonuclear coadaptation underlies fast development in interpopulation hybrids of a marine crustacean. Genome Biol. Evol. 13: evab004.
Healy, T.M., and R.S. Burton. 2020. Strong selective effects of mitochondrial DNA on the nuclear genome. Proc. Natl. Acad. Sci. 117: 6616-6621.
Kofler, R., R.V. Pandey, and C. Schlotterer. 2011. PoPoolation 2: identifying differentiation between populations using sequencing of pooled DNA samples (Pool-Seq). Bioinformatics 27: 3435-3436.
Li, H., and R. Durbin. 2009. Fast and accurate short read alignment with Burrows-Wheeler transform. Bioinformatics 25: 1754-1760.
Lima, T.G. 2014. Higher levels of sex chromosome heteromorphism are associated with markedly stronger reproductive isolation. Nat. Commun. 5: 4743.
Lima, T.G., and C.S. Willett. 2018. Using pool-seq to search for genomic regions affected by hybrid inviability in the copepod *T. californicus*. J. Hered. 109: 469-476.
Lima, T.G., R.S. Burton, and C.S. Willett. 2019. Genomic scans reveal multiple mito-nuclear incompatibilities in population crosses of the copepod *Tigriopus californicus*. Evolution 73: 609-620.
Long, Y., L. Zhao, B. Niu, and Y. Liu. 2008. Hybrid male sterility in rice controlled by interaction between divergent alleles of two adjacent genes. Proc. Natl. Acad. Sci. USA 105: 18871-18876.
Magwene, P.M., J.H. Willis, and J.K. Kelly. 2011. The statistics of bulk segregant analysis using next generation sequencing. PLoS Comput. Biol. 7: e1002255.
Mansfeld, B.N., and R. Grumet. 2018. QTLseqr: an R package for bulk segregant analysis with next-generation sequencing. The plant genome 11: 180006.
Masly, J.P., and D.C. Presgraves. 2007. High-resolution genome-wide dissection of the two rules of speciation in *Drosophila*. PLOS Biol. 5: e243.
Meiklejohn, C.D., M.A. Holmbeck, M.A. Siddiq, D.N. Abt, D.M. Rand, and K.L. Montooth. 2013. An incompatibility between a mitochondrial tRNA and its nuclear-encoded tRNA synthetase compromises development and fitness in *Drosophila*. PLoS Genet. 9: e1003238.
Moyle, L.C., and E.B. Graham. 2005. Genetics of hybrid incompatibility between *Lycopersicon esculentum* and *L. hirsutum*. Genetics 169: 355-373.
Moyle, L.C., and T. Nakazato. 2008. Comparative genetics of hybrid incompatibility: sterility in two *Solanum* species crosses. Genetics 179: 1437-1453.
Muller, H.J. 1942. Isolating mechanisms, evolution and temperature. Biol. Symp. 6: 71-125.

Orr, H.A. 1995. The population genetics of speciation: the evolution of hybrid incompatibilities. Genetics 139: 1805-1813.
Pereira, R.J., T.G. Lima, N. Tessa Pierce-Ward, L. Chao, and R.S. Burton. 2021. Recovery from hybrid breakdown reveals a complex genetic architecture of mitonuclear incompatibilities. Mol. Ecol. 30: 6403 – 6416.
Phillips, B.C., and S. Edmands. 2012. Does the speciation clock tick more slowly in the absence of heteromorphic sex chromosomes? Bioessays 34: 166-169.
Presgraves, D.C. 2008. Sex chromosomes and speciation in *Drosophila*. Trends Genet. 24: 336-343.
Presgraves, D.C., and C.D. Meiklejohn. 2021. Hybrid sterility, genetic conflict and complex speciation: Lessons from the *Drosophila simulans* clade species. Front. Genet. 12: 669045.
Presgraves, D.C., and H.A. Orr. 1998. Haldane's rule in taxa lacking a hemizygous X. Science 282: 952-954.
Price, T.D., and M.M. Bouvier. 2002. The evolution of F1 postzygotic incompatibilities in birds. Evolution 56: 2083-2089.
Sambrook, J., and D.W. Russell. 2006. Purification of nucleic acids by extraction with phenol:chloroform. CSH Protoc. 2006:pdb-prot4455.
Schwann, D.J., R.J. Wang, M.A. White, and B.A. Payseur. 2018. Genetic dissection of hybrid male sterility across stages of spermatogenesis. Genetics 210: 1453-1465.
Slotman, M., A. Torre, and J.R. Powell. 2004. The genetics of inviability and male sterility in hybrids between *Anopheles gambiae* and *An. arabiensis*. Genetics 167: 275-287.
Sweigart, A.L., L. Fishman, and J.H. Willis. 2006. A simple genetic incompatibility causes hybrid male sterility in Mimulus. Genetics 172: 2465-2479.
Tao, Y., S. Chen, D.L. Hartl, and C.C. Laurie. 2003. Genetic dissection of hybrid incompatibilities between *Drosophila simulans* and *D. mauritiana*. I. Differential accumulation of hybrid male sterility effects on the X and Autosomes. Genetics 164: 1383-1398.
Thorvaldsdottir, H., J.T. Robinson, and J.P. Mesirov. 2013. Integrative genomics viewer (IGV): high-performance genomics data visualization and exploration. Brief. Bioinform. 14: 178-192.
Turelli, M., and H.A. Orr. 1995. The dominance theory of Haldane's rule. Genetics 140: 389-402.
Willett, C.S. 2008. No evidence for faster male hybrid sterility in population crosses of an intertidal copepod (*Tigriopus californicus*). Genetica 133: 129-136.

Figures

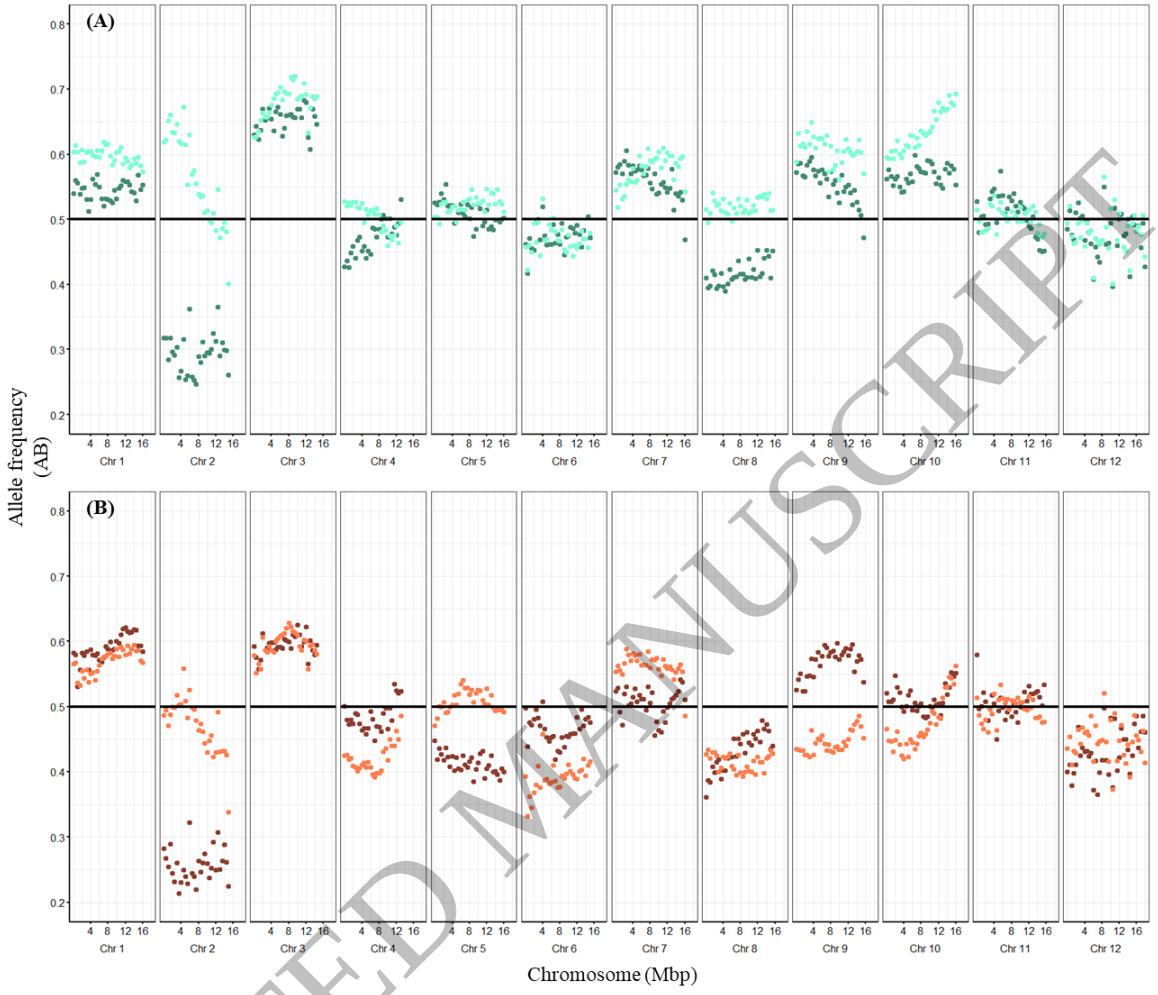

Figure 1. Allele frequencies of fertile and sterile *T. californicus* male F_2 hybrids produced from **(A)** AB♀ x SD♂ and **(B)** SD♀ x AB♂ crosses. Allele frequencies are based on the AB allele perspective. Light-colored symbols are allele frequencies of fertile males; dark-colored symbols are allele frequencies of sterile males. Data points represent mean allele frequency across SNPs in non-overlapping 500 kb sliding windows. Total assembly lengths vary across the 12 *T. californicus* chromosomes (13-18 Mbp).

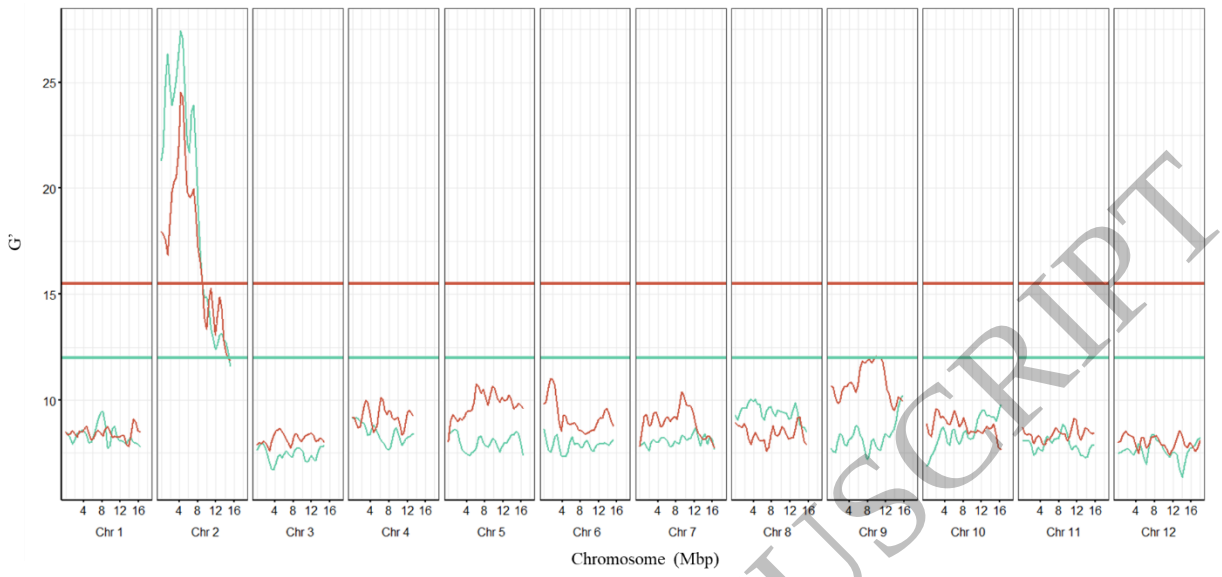

Figure 2. Differences in allele frequencies between fertile and sterile *T. californicus* male F_2 hybrids quantified with the G' statistic. Plot shows smoothed G' values estimated across 1 Mbp windows for AB♀ x SD♂ (teal) and SD♀ x AB♂ (red). Horizontal lines represent statistical thresholds of a genome-wide false discovery rate of 0.01. Total assembly lengths vary across the 12 *T. californicus* chromosomes (13-18 Mbp).

Tables

Table 1. Gene Ontology (GO) biological process terms overrepresented in three QTLs identified on chromosome 2. Allele frequency differences between fertile and sterile F_2 male hybrids were greatest in the region associated with *QTL-2* in both cross directions. Only the five most significant terms in each QTL with at least ten genomic annotations included (see Table S3 for complete list).

Gene ontology term (Region on Chromosome 2)	GO term ID	Genomic annotations	Expected regional	Regional annotations	p-value
QTL-1 (0.8 – 2.4 Mbp)					
Cellular response to manganese ion	0071287	10	0.06	2	0.002
DNA ligation	0006266	10	0.06	2	0.002
Maintenance of protein localization in endoplasmic reticulum	0035437	15	0.09	2	0.004
Nucleotide-excision repair, DNA duplex unwinding	0000717	15	0.09	2	0.004
Regulation of endoplasmic reticulum unfolded protein response	1900101	16	0.1	2	0.004
QTL-2 (3.4 – 5.7 Mbp)					
Spermatogenesis	0007283	107	2.15	9	< 0.001
Protein ubiquitination	0016567	411	8.27	21	0.001
Ubiquitin-dependent protein catabolic process	0006511	310	6.24	14	0.004
Phosphatidylinositol phosphorylation	0046854	17	0.34	3	0.004
Phosphatidylinositol biosynthetic process	0006661	56	1.13	5	0.005
QTL-3 (6.2 – 7.6 Mbp)					
Negative regulation of actin filament depolymerization	0030835	21	0.26	3	0.002
Regulation of hydrolase activity	0051336	525	6.54	15	0.002
Substrate adhesion-dependent cell spreading	0034446	57	0.71	6	0.002
Histone monoubiquitination	0010390	25	0.31	3	0.004
Regulation of intracellular steroid hormone receptor signaling pathway	0033143	58	0.72	4	0.006